Wiley Online Library
Early View publication on www.wileyonlinelibrary.com
(issue and page numbers not yet assigned;
citable using Digital Object Identifier – **DOI**)

J. Biophotonics 1–5 (2014) / **DOI** 10.1002/jbio.201300208

Journal of BIOPHOTONICS

LETTER

A new filtering technique for removing anti-Stokes emission background in gated CW-STED microscopy

Ivàn Coto Hernàndez[1,2], *Chiara Peres*[1,2], *Francesca Cella Zanacchi*[1], *Marta d'Amora*[1], *Sotirios Christodoulou*[3], *Paolo Bianchini*[1], *Alberto Diaspro*[*,1,2], *and Giuseppe Vicidomini*[*,1]

[1] Nanophysics, Istituto Italiano di Tecnologia, Via Morego 30, 16136, Genoa, Italy
[2] Department of Physics, University of Genoa, Via Dodecaneso 33, 16146 Genoa, Italy
[3] Nanochemistry, Istituto Italiano di Tecnologia, Via Morego 30, 16136, Genoa, Italy

Received 28 December 2013, revised 24 February 2014, accepted 24 February 2014
Published online 18 March 2014

Key words: fluorescence microscopy, stimulated emission depletion (STED) microscopy, super-resolution microscopy, background subtraction

Supporting information for this article is available free of charge under: http://dx.doi.org/10.1002/jbio.201300208

Stimulated emission depletion (STED) microscopy is a prominent approach of super-resolution optical microscopy, which allows cellular imaging with so far unprecedented unlimited spatial resolution. The introduction of time-gated detection in STED microscopy significantly reduces the (instantaneous) intensity required to obtain sub-diffraction spatial resolution. If the time-gating is combined with a STED beam operating in continuous wave (CW), a cheap and low labour demand implementation is obtained, the so called gated CW-STED microscope. However, time-gating also reduces the fluorescence signal which forms the image. Thereby, background sources such as fluorescence emission excited by the STED laser (anti-Stokes fluorescence) can reduce the effective resolution of the system. We propose a straightforward method for subtraction of anti-Stokes background. The method hinges on the uncorrelated nature of the anti-Stokes emission background with respect to the wanted fluorescence signal. The specific importance of the method towards the combination of two-photon-excitation with gated CW-STED microscopy is demonstrated.

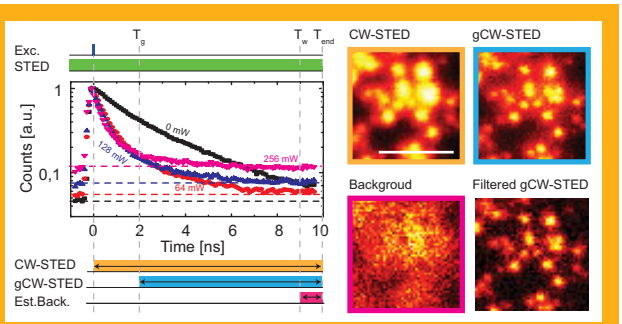

Principle and time course of the measurement for the proposed anti-Stokes emission background subtraction method (right). Application of the method for a fluorescent beads calibration sample (left).

Two decades from its invention [1], stimulated emission depletion (STED) microscopy has reached a level of maturity that has led to routine applications in life sciences [2]. This has been achieved following several advancements, such as the improved laser technologies, the design of new highly photostable

* Corresponding author: e-mail: alberto.diaspro@iit.it and giuseppe.vicidomini@iit.it.

fluorophores, the realization of new optical architectures for multidimensional (x, y, z, t, λ) imaging and the understanding of the photo-physics of a fluorophore when subjected to the STED laser light. As an example, gated-STED (gSTED) microscopy has been developed. It is easy to demonstrate that the later the fluorescence signal of a fluorophore is observed, with respect to its excitation event, the more likely it becomes that it is inhibited if it is continuously exposed to stimulating photons [3, 4]. In particular, measuring the fluorescence after a time T_g, from the excitation events, ensures that the signal stems from fluorophores which have resided in the excited-state for at least a time T_g and thereby, in the presence of the STED beam, have been exposed to stimulating photons for at least the same time. Although this notion was known since the first STED microscopy implementation [5] and was also later experimentally demonstrated [6], its application for reducing the required STED beam intensity and for simplifying the implementation of a STED microscope has emerged only recently [7, 8]. By applying a pulsed excitation beam together with a STED beam operating in continuous wave (CW) and a time-gated detection, the fluorescence on-off contrast, i.e. the probability of inhibiting a fluorophore for a given STED beam intensity, is improved. Hence, this implementation, usually called gated CW-STED (gCW-STED) microscopy, provides subdiffraction resolution using moderate light intensity and thereby reduces photodamage effects [7].

Theoretically, the image contrast, thereby the effective spatial resolution, of a gCW-STED microscope can be continuously increased by delaying the detection [3, 4], but the decrease in wanted signal caused by the time-gating imposes an upper limit on the choice of T_g. In the presence of background, long T_g can induce a strong reduction of the signal-to-background ratio (SBR) which cancels out the benefits of time-gating and in the worst case reduces the effective resolution [4]. Certainly, by increasing the intensity of the excitation beam the wanted signal can improved. However, this option is limited by the photodamage effects, and by the saturation of the fluorescence emission, so the removal of the background signal is the best choice for restoring the benefit of time-gating.

A potential source of background in STED microscopy is the signal induced by the STED beam itself. Ideally, the STED beam forces the excited fluorophores to emit photons (stimulated emission) at the same wavelength as the beam, which can be specifically blocked by appropriate spectral filters and allowing most of the spontaneous emission (fluorescence) to pass.

Thereby, when the STED beam is shaped as a doughnut and coaligned with a regular Gaussian excitation beam, it transiently inhibits the fluorescence of all fluorophores in the focal excitation region except those located in a tiny, subdiffraction-sized region around the doughnut center. Scanning the coaligned beams across the specimen yields images with subdiffraction spatial resolution. Practically, the STED beam can induce other processes, which can lead to the emission of an higher energy photon (anti-Stokes emission) not blocked by the spectral filters. In terms of imaging, the fluorophores on the doughnut crest are not completely switched-off, but they contribute, together with the fluorophores located in the doughnut center, to form the image. Infact, if the fluorescent signal coming from the doughnut center is comparable with this anti-Stokes emission background, the contrast of the image is reduced. Of course, anti-Stokes emission evoked by the STED beam can be reduced by red-shifting the wavelength of the STED laser, where the absorption cross-section of the fluorophore and thus the anti-Stokes fluorescence decrease. However, the stimulated emission cross-section decreases as well, and the intensity of the STED laser has to be increased to induce a comparable depletion.

Since the anti-Stokes fluorescence background is triggered solely by the STED beam, it has been recently demonstrated that a lock-in (synchronous) detection system can effectively subtract this background [9, 10]. *Per contra*, when the lock-in detection is applied for imaging, it doubles the recording time. That is each pixel needs two equal time measurements: (i) the open phase, where excitation and STED beams are applied (as for conventional imaging) and the signal induced by both beams is collected; (ii) the closed phase, where only the STED beam is applied, thereby only the signal induced by the STED beam is collected. In essence, by subtracting the closed signal from the open signal, the lock-in retrieves the signal induced by the excitation beam only. Notably, longer recording time increases phototoxicity effects. Further, when working with fluorophores with non-negligible triplet build-up, the irradiation with the STED beam during the closed phase can increase the photodamage [11].

Here we show that in the case of gCW-STED microscopy implemented with a time-correlated-single-photon-counting (TCSPC), by considering the histogram of the photon arrival time (also called decay curve) the anti-Stokes fluorescence background can be removed without the lock-in detection, namely without the closed phase measurement.

Figure 1(a) shows the so called depletion curves (or fluorescent on-off contrast) in the case of Oregon Green 488-labelled antibody (see Supplementary Information for details about the sample preparation and the gCW-STED microscope, Suppl. Figure 1) and 560 nm STED beam. If we denote with $T_1 = [T_g, T_{end}]$ the time-gate, the raw depletion curve is equal to the fraction to which the gated

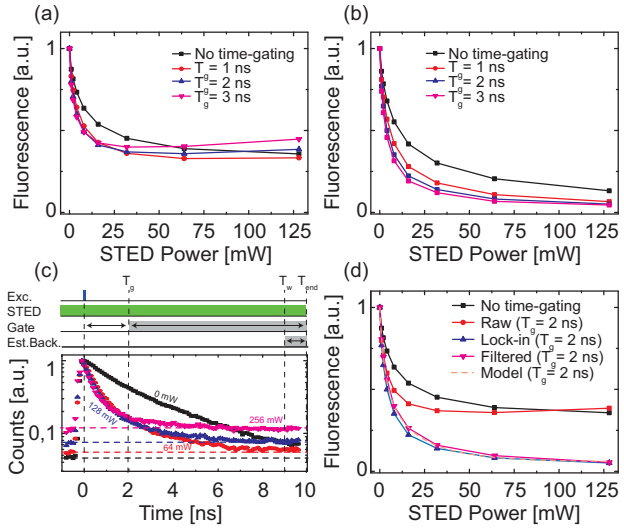

Figure 1 Principle and validation of the proposed filter to remove the anti-Stokes emission background. (**a**) Raw depletion curves of Oregon Green 488-labeled antibody for different delay-time $T_g = 0$, 1, 2, 3 ns. (**b**) Recovered depletion curves using a lock-in detection for different delay-time $T_g = 0$, 1, 2, 3 ns. (**c**) TCSPC histogram of the signal measured at different STED beam powers P_{STED} together with the time course of the measurement (top). Time bin width of the TCSPC histogram 100 ps. The dash lines represent the minimum values for each histogram. (**d**) Recovered depletion curve using the proposed filter for $T_g = 2$ ns, $\lambda_{STED} = 560$ nm, $\lambda_{exc} = 488$ nm, $P_{exc} = 15$ µW, $\Delta T_2 = 500$ ps and time bin width 100 ps.

fluorescence FT_1 is suppressed by the STED beam as a function of the power P_{STED}, i.e. $\eta_{raw}(P_{STED}) = FT_1(P_{STED})/FT_1(PT_{STED} = 0)$. The conventional ($T_g = 0$ ns) depletion curve shows a residual fluorescence signal of 35% also at high STED beam power ($P_{STED} = 125$ mW). This residual signal is mostly linked to the non-negligible probability of exciting the fluorophore at 560 nm (see Supplementary Information for Oregon Green 488 excitation spectrum, Suppl. Figure 2). When time-gating ($T_g > 0$ ns) is applied the efficiency of depletion increases at low STED beam power, but at high STED beam power it decreases. The depletion enhancement associated with the time-gated detection is canceled-out by the anti-Stokes fluorescence background which increases for increasing STED beam powers. The efficiency of depletion further deteriorates for higher delay-time T_g since the anti-Stokes fluorescence background decreases linearly with the delay-time T_g but the wanted fluorescence signal decreases exponentially [4]. The ability of time-gated detection to enhance the depletion was fully restored by using a lock-in detection scheme (Figure 1(b)). In this case, we subtracted the gated closed phase signal $FT_1^c(P_{STED})$ from the gated "open" phase signal $FT_1(P_{STED})$, i.e. $\eta_{lock-in}(P_{STED} = (FT_1(P_{STED}) - FT_1^c(P_{STED}))/FT_1(P_{STED} = 0)$. However, the doubling of the the acquisition and exposure times linked to the lock-in detection can increase the photodamage effects.

By exploring the arrival time of the photons on the detector, we propose an equivalent method which does not need the doubling of the acquisition time. Since the anti-Stokes fluorescence photons (in general any photons induce solely by the STED beam) are generated by a CW beam, those photons will appear in the decay curve as a uniform and uncorrelated (with respect to the excitation pulses) background (Figure 1(c)). Hence, to recover the pure fluorescence decay curve induced solely by the excitation beam, from the decay curve its minimum value can be subtracted. Whilst this approach works well in the case of high counts, it could underestimate the background in the case of low counts. To reduce the possibility of underestimating the background, the number of photons to be subtracted is obtained by averaging the values measured in a small amount of late-bins $T_2 = [T_w, T_{end}]$ in the histogram, where the probability of counting photons induced by the excitation beam is negligible. Early-bins before the excitation events can be used as well. Figure 1(d) compares the depletion curves obtained applying the lock-in method with the proposed digital filtering approach. Namely, $\eta_{filt.}(P_{STED}) = (FT_1(P_{STED}) - \beta FT_2(P_{STED}))/(FT_1(P_{STED} = 0) - \beta FT_2(P_{STED} = 0))$, where β denotes the ratio between the width of the two time-gates, $\Delta T_1/\Delta T_2$. Almost no differences can be observed between the two methods, but the digital filtering method halves both the recording time and the STED beam irradiation. Notably, the filtered depletion curve can be well described by our model (dash line Figure 1(b), see Supplementary Information for the description of the model, Suppl. Figure 3). It should be noted that the width of ΔT_2 has to be carefully adjusted. If ΔT_2 equals the histogram bin-width, it can underestimate the background, but larger ΔT_2 can lead to the subtraction of wanted fluorescence late photons (see Suppl. Figure 4), which according to time-gating theory contains the high resolution information [4].

When we applied the proposed filter to the decay curves of each individual pixel, the contrast of the image improved. Figure 2(a) shows gCW-STED imaging of sub-diffraction sized fluorescent beads for increasing STED beam power P_{STED} and increasing detection delay T_g. The contrast and thereby the effective spatial resolution improve when the STED beam power increases (from top to bottom) and when a small detection delay is used $T_g = 1$ ns, but for longer detection delay $T_g = 2$ ns, the anti-Stokes emission background is not negligible and hides the expected effective resolution improvement. The ef-

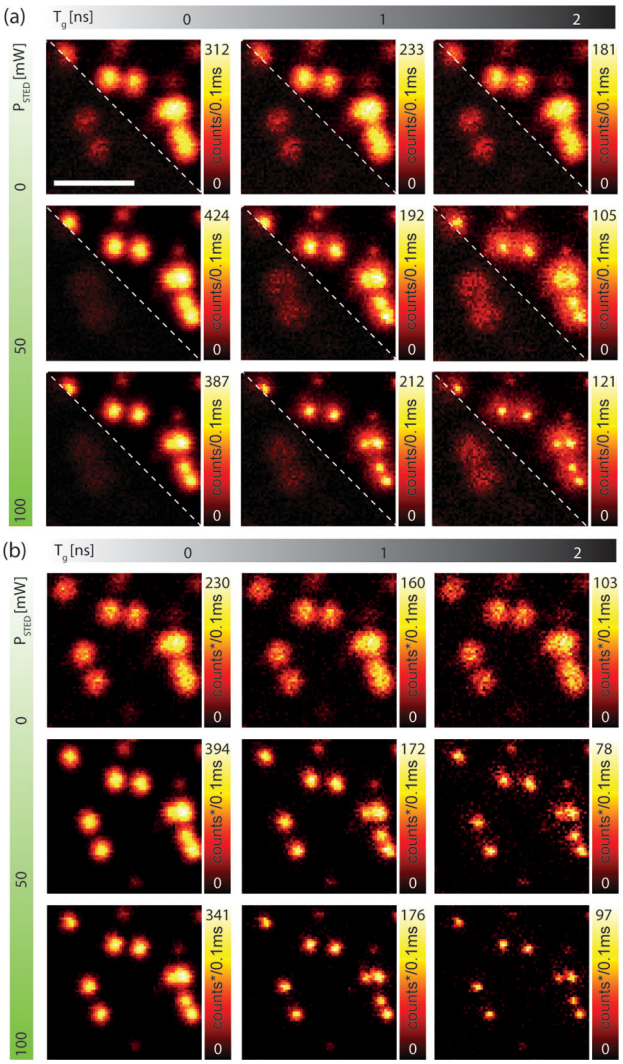

Figure 2 Comparison between raw (**a**) and filtered (**b**) gCW-STED imaging of fluorescent beads for increasing STED beam power P_{STED} and time-delay T_{g}. $\Delta T_2 = 500$ ps, time bin width 100 ps, $\lambda_{\mathrm{exc}} = 488$ nm, $P_{\mathrm{exc}} = 10\,\mu$W and $\lambda_{\mathrm{STED}} = 560$ nm. The lower left corners show the anti-Stokes excitation background images in the same color look-up table of the raw images. The asterisk in the color look-up table denotes that the negative counts obtained after filtering are clipped to zero. Scale bar: 1 μm.

fective resolution is fully recovered when we applied the proposed filter (see Figure 2(a)).

The benefit of the filter became more evident when we observed convoluted structures, like the tubulin network of a cell. Figure 3(a) shows the tubulin filaments of an HeLa cell immunolabeled with Oregon Green 488. Almost no improvement in the effective resolution can be observed between confocal and CW-STED ($T_{\mathrm{g}} = 0$ ns) images, as well as, between CW-STED and gCW-STED ($T_{\mathrm{g}} = 0$ ns) images, but sub-diffraction details are recovered when the anti-Stokes fluorescence background is filtered-out from the gCW-STED image. Figure 3(b) compares the same imaging modalities when Alexa 488 substitutes Oregon Green 488. In this case the SBR ratio of the original gCW-STED image is higher (see Supplementary Information for Oregon Green 488 and Alexa 488 spectral comparison, Suppl. Figure 2), however the advantage of using the digital filter is still evident. It should be emphasized that imaging of Oregon Green 488 and Alexa 488 labelled samples are usually performed with yellow STED beams (577 nm or 592 nm) which reduce the anti-Stokes fluorescence emission, thereby the proposed filtering method improves the versatility of the gCW-STED microscope. As a matter of fact, the portfolio of compatible fluorophores for a given STED beam wavelength increases. We finally anticipate that the proposed method is fundamental when gCW-STED microscopy is combined with two-photon-excitation (2PE) (see Supplementary Information for details about the gated 2PE-CW-STED microscope, Suppl. Figure 5, where, due to the small 2PE cross-section, the fluorescence signal is particularly weak [12]. Even if we shifted the STED beam wavelength to 577 nm, the resolution enhancement

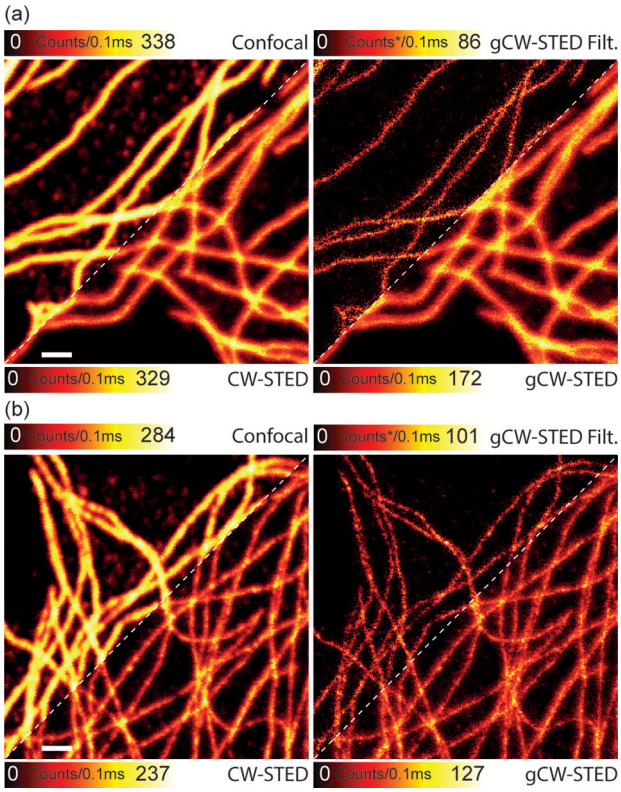

Figure 3 Comparison between confocal, CW-STED, raw and filtered imaging of microtubules of fixed HeLa cells immunolabelled with Oregon Green (**a**) and Alexa 488 (**b**). $\lambda_{\mathrm{STED}} = 560$ nm, $P_{\mathrm{STED}} = 40$ mW, $T_{\mathrm{g}} = 1$ ns, $\Delta T_2 = 500$ ps, time bin width 100 ps, $\lambda_{\mathrm{exc}} = 488$ nm and $P_{\mathrm{exc}} = 10\,\mu$W. Scale bars: 1 μm.

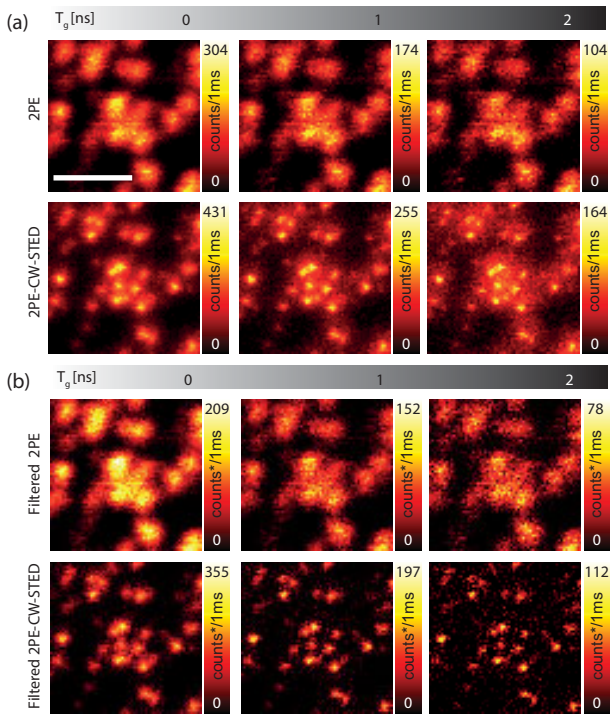

Figure 4 Comparison between raw (**a**) and filtered (**b**) gCW-STED imaging of 40 nm fluorescent beads under two-photon-excitation regime. $\lambda_{STED} = 577$ nm, $P_{STED} = 50$ mW, $T_g = 1$ ns, $\Delta T_2 = 500$ ps, time bin width 100 ps, $\lambda_{2PE} = 760$ nm and $P_{exc} = 9$ mW. Scale bar: 1 μm.

expected from 2PE-gCW-STED becomes relevant only when we applied the proposed filter (see Figure 4). The method represents an important step towards the implementation of an efficient but also cheap and low-complex implementation of 2PE-STED microscopy [13, 14].

We have presented and validated a new method for compensating the SBR reduction associated with the time-gated detection of a gCW-STED microscope. The method subtracts any form of anti-Stokes emission background induced independently by the STED beam. It can be a valuable alternative to lock-in techniques, since it removes the need for the "closed" phase measurement, thereby reducing the recording time and the sample irradiation, i.e. reducing the photodamage and the phototoxicity. Our implementation is based on a TCSPC card, which is commonly used in gCW-STED microscopy [8, 15], but an alternative implementation can use two hardware time-gates. Similarly to the lock-in detection methods the success of the proposed method depends on the reliability of the background estimation, which increases with the increase of the pixel dwell-time [9]. Thereby, as with the the lock-in methods, this method also needs the careful choice of the pixel dwell-time. Further, the background estimation degrades when the unperturbed lifetime of the fluorophore approaches the pulse interval of the excitation laser. In any case, the most used fluorophores have a lifetime of 1–5 ns, which makes the method compatible with the typical 80 MHz repetition rate (12.5 ns pulse interval) of the laser sources used in STED and 2PE-STED microscopy.

Acknowledgements: We thank Dr. Benjamin Harke and Jenu Chacko for fruitful discussions. We also thank Eileen Sheppard for proofreading the manuscript. This work was supported in part by the Italian Ministry of Education, University and Research (MIUR) through PRIN project N. 2008S22MJC 005.

References

[1] S. W. Hell and J. Wichmann, Opt. Lett. **19**, 780–782 (1994).
[2] T. Mueller, C. Schumann, and A. Kraegeloh, ChemPhysChem **13**, 1986–2000 (2012).
[3] J. R. Moffitt, C. Osseforth, and J. Michaelis, Opt. Express **19**, 4242–4254 (2011).
[4] G. Vicidomini, A. Schönle, H. Ta, K. Y. Han, G. Moneron, C. Eggeling, and S. W. Hell, PLoS ONE **8**, e54421 (2013).
[5] S. W. Hell, S. Jakobs, and L. Kastrup, Appl. Phys. A: Mater. Sci. Process. **77**, 859–860 (2003).
[6] E. Auksorius, B. R. Boruah, C. Dunsby, P. M. P. Lanigan, G. Kennedy, M. A. A. Neil, and P. M. W. French, Opt. Lett. **33**, 113–115 (2008).
[7] G. Vicidomini, G. Moneron, K. Y. Han, V. Westphal, H. Ta, M. Reuss, J. Engelhardt, C. Eggeling, and S. W. Hell, Nat. Methods **8**, 571–573 (2011).
[8] G. Vicidomini, I. Coto Herńandez, M. d'Amora, F. Cella Zanacchi, P. Bianchini, and A. Diaspro, Methods, doi:10.1016/j.ymeth.2013.06.029.
[9] G. Vicidomini, G. Moneron, C. Eggeling, E. Rittweger, and S. W. Hell, Opt. Express **20**, 5225–5236 (2012)
[10] E. Ronzitti, B. Harke, and A. Diaspro, Opt. Express, **21**, 210–219 (2013).
[11] J.-i. Hotta, E. Fron, P. Dedecker, K. P. F. Janssen, C. Li, K. Müllen, B. Harke, J. Bückers, S. W. Hell, and J. Hofkens, JACS **132**, 5021–5023 (2010).
[12] A. Diaspro, P. Bianchini, G. Vicidomini, M. Faretta, P. Ramoino, and C. Usai, Biomed. Eng. Online **5**, 36 (2006).
[13] P. Bethge, R. Chereau, E. Avignone, G. Marsicano, and U. Nagerl, Biophys. J. **104**, 778–785 (2013).
[14] K. T. Takasaki, J. B. Ding, and B. L. Sabatini, Biophys. J. **104**, 770–777 (2013).
[15] Y. Wang, C. Kuang, Z. Gu, Y. Xu, S. Li, X. Hao, and X. Liu, Opt. Eng. **52**, 093107–093107 (2013)